Journal of Power Sources 218 (2012) 79–87

Contents lists available at SciVerse ScienceDirect

Journal of Power Sources

journal homepage: www.elsevier.com/locate/jpowsour

Degradation analyses of $Ru_{85}Se_{15}$ catalyst layer in proton exchange membrane fuel cells

Qiaoming Zheng [a], Xuan Cheng [a,b,*], Ting-Chu Jao [c,d], Fang-Bor Weng [c,d,**], Ay Su [c,d], Yu-Chun Chiang [c,d]

[a] Department of Materials Science and Engineering, Xiamen University, Xiamen 361005, Fujian, China
[b] Fujian Key Laboratory of Advanced Materials, Xiamen University, Xiamen 361005, Fujian, China
[c] Department of Mechanical Engineering, Yuan Ze University, Zhongli 320, Taoyuan, Taiwan
[d] Fuel Cell Center, Yuan Ze University, Zhongli 320, Taoyuan, Taiwan

HIGHLIGHTS

- The lowest performance loss of 44% obtained with 0.27 mg Ru cm^{-2} and 33% Nafion.
- Degradation mechanism of MEAs with $Ru_{85}Se_{15}$ catalysts in fuel cells.
- Effects of Ru and Nafion loads in the catalyst layer on cell degradation.
- The dissolutions and migrations of Se and Ru proved by SEM, HRTEM and EDX analyses.

GRAPHICAL ABSTRACT

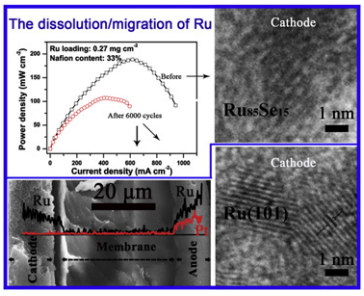

ARTICLE INFO

Article history:
Received 5 April 2012
Received in revised form
17 June 2012
Accepted 21 June 2012
Available online 28 June 2012

Keywords:
Proton exchange membrane fuel cells
Selenium modified ruthenium
Nafion content
Ru load
Accelerated degradation tests

ABSTRACT

Accelerated degradation tests (ADTs) for the H_2/air single cell are carried out at 65 °C and ambient pressure by cycling the cell between 0 and 200 mA cm^{-2} up to 6000 cycles. Membrane electrode assemblies (MEAs) are prepared using the Nafion 212 membrane and the carbon supported platinum as an anode catalyst, as well as the carbon supported $Ru_{85}Se_{15}$ as a cathode catalyst prepared with five selected Nafion contents and Ru loads to represent the optimized (33% Nafion and 0.27 mg Ru cm^{-2}), overloaded (43% Nafion and 0.61 mg Ru cm^{-2}) and underloaded (20% Nafion and 0.14 mg Ru cm^{-2}) conditions. The lowest cell performance loss of 44% in terms of peak power density is achieved with 33% Nafion and 0.27 mg Ru cm^{-2}. Very severe losses of 80% and 82% are found for 20% and 43% Nafion contents, respectively, while relatively moderate losses of 57% and 64% for 0.14 and 0.61 mg Ru cm^{-2}, respectively. Dissolution and migration of Se/Ru and corrosion of carbon support from the catalyst, together with the shrinkage and release of sulfonic acid from the membrane are identified and correlated to decayed cell performances.

1. Introduction

Proton exchange membrane (PEM) fuel cells are considered as a most promising clean power source due to their high specific power densities and relatively low operating temperatures [1]. However, the cost of membrane electrode assemblies (MEAs), in particular, the use of platinum based catalysts, is a vital issue for fuel cell application. An equally important technical barrier for fuel cells as a practical power source is durability under a wide range

* Corresponding author. Department of Materials Science and Engineering, Xiamen University, Xiamen 361005, Fujian, China. Tel.: +86 592 218 5599; fax: +86 592 218 3937.
** Corresponding author. Department of Mechanical Engineering, Yuan Ze University, Zhongli 320, Taoyuan, Taiwan. Tel.: +886 3 4618691; fax: +886 3 4555574.
E-mail addresses: zhengqiaom@xmu.edu.cn, xcheng@xmu.edu.cn (X. Cheng), fangbor@saturn.yzu.edu.tw (F.-B. Weng).

0378-7753/$ – see front matter © 2012 Elsevier B.V. All rights reserved.
http://dx.doi.org/10.1016/j.jpowsour.2012.06.076

of operational conditions, especially dynamic load cycling and start-up/shut-down, which provide significant challenges for fuel cell application [2]. Selenium modified ruthenium (Ru_xSe_y) catalysts are considered as potential alternatives to platinum based cathode catalysts, due to their better selectivity toward the oxygen reduction reaction (ORR), lower cost and high abundance of ruthenium as compared to platinum [3]. These cathode catalysts have attracted more and more attention since Alonso-Vante [4], for the first time, reported Chevrel-phase $Ru_2Mo_4Se_8$ catalysts showing a comparable ORR activity in 0.5 mol dm^{-3} H_2SO_4 to Pt catalysts in 1986. In the past 25 years, Ru_xSe_y catalysts have been extensively investigated from the development of synthesis methods to the catalytic mechanism toward ORR, and performance evaluation in fuel cells. The carbon supported $Ru_{85}Se_{15}$ catalyst, synthesized via a microwave-assisted polyol process, showed the breakthrough maximum power density of 400 mW cm^{-2} at 1300 mA cm^{-2} using a relatively high Ru load of 0.4 mg cm^{-2} and Pt load of 0.3 mg cm^{-2} in H_2/O_2 fuel cells at 80 °C under the back pressure of 0.2 MPa for both anode and cathode [5]. However, the current density of $Ru_{85}Se_{15}$/C was 200 mA cm^{-2} at 0.6 V, which is much lower than that of Pt/C (1800 mA cm^{-2} at 0.6 V) [5]. Therefore, the challenges for the improvement in fuel cell performance of Ru_xSe_y catalysts still remain to not only discover new chalcogenide electrocatalyst compositions, design catalyst structure, develop novel synthesis methods and novel substrates for preparing catalysts, but also prepare the MEAs and optimize the operation conditions of fuel cells. Similar to Pt-based catalysts, the cell performance of Ru_xSe_y catalysts could be significantly enhanced by optimizing operating parameters, such as proper electrode preparisons, uses of back pressures and higher operating temperature. Our previous study [6] demonstrated that the well dispersed $Ru_{85}Se_{15}$ nanoparticles on citric acid treated supports could be prepared using the microwave assisted polyol method at the optimized solution pH of 7. Using lower loading of 0.14 mg Ru cm^{-2}, the maximum power densities for the multi-walled carbon nanotubes (MWCNTs) supported and commercial carbon (XC-72R) supported $Ru_{85}Se_{15}$ catalysts were 166 mW cm^{-2} and 126 mW cm^{-2}, respectively, while suffering the performance losses of 38% and 64% in terms of the maximum power densities, respectively, upon 6000 cycle degradation in the H_2/air single cells [6]. When further optimizing the MEA fabrication with 0.27 mg Ru cm^{-2} and 33% Nafion, the maximum peak power densities of 190 mW cm^{-2} (a 50% higher) could be achieved with carbon (XC-72R) supported $Ru_{85}Se_{15}$ at the same fuel cell operation [7]. The maximum power density measured at 80 °C in the H_2/O_2 single cell using the Ru_xSe_y as a cathode catalyst was almost doubled to those obtained at 40 °C [8]. Up to now, Ru_xSe_y catalysts have shown lower cell performance compared with Pt-based catalysts in PEM fuel cells. Further improvements in catalytic activity are urgently required in order to compete with Pt-based catalysts. However, Ru_xSe_y catalysts could be possibly applied in direct methanol fuel cells due to their comparable ORR performance and high methanol tolerance, especially in a high concentration methanol fuel cell. The $Ru_{85}Se_{15}$/C catalyst displayed excellent methanol tolerance in O_2-saturated methanol-containing 0.5 mol dm^{-2} H_2SO_4 solutions [5]. The maximum power density of 45 mW cm^{-2} was achieved with RuSe/CNT using 6 mol dm^{-3} methanol fuel, which is more than three times higher than that incorporated with Pt/C in the methanol/air single cell [9].

In addition to activity and selectivity, durability of catalysts is even more critical in determining cell performance. However, the degradation behaviors of $Ru_{85}Se_{15}$ with respect to the Nafion contents and Ru loads in the single cell tests were little investigated. The degradation mechanism of $Ru_{85}Se_{15}$ under the fuel cell test remains unclear. Various degradation mechanisms of MEAs with platinum based catalysts have been examined in PEM fuel cells by different operational conditions [10–13]. The degradation of MEAs may be mainly caused by loss of catalyst activity due to sintering or migration of platinum particles on the carbon support, detachment and dissolution of platinum into the electrolyte, corrosion of carbon support, deteriorated membrane and contamination of impurities. More comprehensive reviews of the degradation mechanism of platinum based MEAs can be found elsewhere [2,14,15]. However, the degradation behaviors of fuel cells with non-platinum based MEAs are little studied. It was found that the citric acid-treated MWCNTs supported $Ru_{85}Se_{15}$ catalysts exhibited better cell performance and durability than carbon supported $Ru_{85}Se_{15}$ due to the higher degree of graphitization [6]. Xu et al. [16] concluded that the introduction of TiO_2 into carbon support could prevent Se dissolution and reduce Ru dissolution from $Ru_{85}Se_{15}$/TiO_2/C based on the ICP analysis of tested solutions after 1000 potential cycles between 0 V and 1 V. They suspected that this might be responsible for the 18% less performance loss in terms of maximum peak power density tested in the H_2/O_2 fuel cells at 80 °C under 0.2 MPa back pressure [16]. However, no experimental evidence has been provided in fuel cell tests.

In this study, the degradation behaviors of carbon supported $Ru_{85}Se_{15}$ catalyst were examined by performing a series of H_2/air single cell tests using the MEAs fabricated by the ultrasonic spray technique with selected Nafion contents and Ru loads in the cathode catalyst layers. The physical and chemical characteristics of MEAs before and after the 6000 cycle degradation were investigated by the EIS, SEM/EDX, HRTEM/SAED, Raman and FTIR techniques. Possible degradation mechanisms of $Ru_{85}Se_{15}$ are discussed based on the experimental observations.

2. Experimental

2.1. Single cell tests

Anode catalyst ink was prepared by mixing 40% Pt/C (Johnson Matthey) and 5% Nafion solutions with the ethanol and then sonicating for 30 min. The $Ru_{85}Se_{15}$ catalysts were prepared with citric acid (CA) treated commercial carbon blacks Vulcan XC-72R (Cabot Corp., BET: 237 m^2 g^{-1}) using the microwave assisted polyol synthesis method at the optimized initial solution pH = 7 as determined previously [6]. While 25% $Ru_{85}Se_{15}$/C and 5% Nafion solutions were well distributed in ethanol and used as the cathode ink. The membrane electrode assemblies (MEAs) were fabricated by the catalyst coated membrane method using the ultrasonic-spray instrument as described previously [7]. The anodes of MEAs were prepared with 0.26 mg cm^{-2} Pt and 33% Nafion content, which was in term of wt% of Nafion (dry weight of Nafion ionomer divided by the total weights of the catalyst and Nafion ionomer, multiplied by 100). And the various Ru loads (0.14, 0.27, 0.61 mg cm^{-2}) and Nafion contents (20, 33, 43%) were used in the cathode layers.

Single cells with area of 5 cm^2 were assembled with catalyst coated membranes, Teflon gaskets and two GDLs (SGL carbon AG, Germany). Hydrogen and air with flow rates of 100 and 250 ml min^{-1} were fed to the anode and cathode, respectively. The polarization curves were measured using a fuel cell test station (850C, Scribner Associates Inc.) at 65 °C under ambient pressure. In order to examine the stability of the catalysts, the accelerated degradation tests (ADTs) were performed at identical testing conditions. The cell performance was first investigated before the ADTs. A load by cycling between 0 and 200 mA cm^{-2} was applied for different cycles. The polarization measurement was obtained after each 1000 cycles up to 6000 cycles. After the polarization measurements, the single cell was stabilized at 0.4 V for 10 min and the impedance measurements were made at 0.4 V with a frequency

range of 10 kHz ~ 0.1 Hz. The data were curve-fitted with ZSimpWin software (Princeton Applied Research) utilizing the complex non-linear least square errors technique.

2.2. Characterizations of MEAs

The carbon supported $Ru_{85}Se_{15}$ catalyst, pure Nafion 212 membrane and the cathode of MEAs including the membrane were characterized by a TriVista CRS557 Raman instrument (Princeton Instruments) using the Ultra-Violet 325 nm wavelength from 500 cm^{-1}–1800 cm^{-1}. The surface and cross-sectional morphologies of MEAs before and after the ADT were obtained by cutting the MEAs in liquid nitrogen and using a LEO1530 field emission scanning electron microscope (Oxford Instrument, Germany). The corresponding elemental compositions were measured by the build-in energy dispersive X-ray (EDX) spectroscope.

The cathode catalysts were scraped off from the MEAs and then dispersed well in ethanol. A drop of the catalyst suspension with ethanol was placed on a carbon-coated copper grid and analyzed using high resolution transmission electron microscope (HRTEM) (JEM-2100, JEOL, Japan) operating at 200 kV.

FTIR-ATR (Avatar 360, Thermo Nicolet Corporation) measurements were carried out for fresh and degraded Nafion membranes. The spectra were collected after 64 scans for the background in a range of 1500–850 cm^{-1}. To separate membrane from MEAs, the MEA samples were immersed in isopropyl alcohol and water, and then were gently wiped to remove the catalyst layer. The membrane was washed several times with water and dried before analysis.

3. Results and discussion

3.1. Lifetime performance of fuel cell

The cell performances with different Nafion contents and Ru loads in the cathode catalyst layer have been previously investigated in the H_2/air single cells at 65 °C under ambient pressure [7]. It was found that the optimized Ru loads were less than 0.8 mg Ru cm^{-2} with 33% Nafion contents. The maximum peak power density of 190 mW cm^{-2} and the best catalyst utilization of 917 mW $(mg\ Ru)^{-1}$ could be achieved at 0.27 and 0.14 mg Ru cm^{-2}, respectively, with 33% Nafion [7]. The fuel cell performances before and after the ADTs corresponding to the maximum peak power density and the best catalyst utilization are presented in Fig. 1. As evident in Fig. 1(a), with optimized 0.27 mg Ru cm^{-2} and 33% Nafion, the more significant performance degradation was observed at the first 1000 cycles. The cell performance decayed gradually with the increases in cycle numbers and eventually remained almost unchanged upon 6000 cycles. In the case of 0.14 mg Ru cm^{-2} and 33% Nafion (Fig. 1(b)), the most severe degradation also occurred at the first 1000 cycles. Although the catalyst utilization was better than that using 0.27 mg Ru cm^{-2}, the lifetime performance using lower Ru loading became much worse, in particular, at higher current densities.

To further distinguish the effects of Ru and Nafion loads on lifetime performance, the polarization and power density curves were obtained in the H_2/air fuel cells under the same operating conditions including sweep rate, humidity and temperature for the two selected Nafion contents and Ru loads, which represent overloaded (43% Nafion and 0.61 mg Ru cm^{-2}) and underloaded (20% Nafion and 0.14 mg Ru cm^{-2}) conditions. The results are shown in Fig. 2. Clearly, with 0.27 mg Ru cm^{-2} (Fig. 2(a–b)), the cell performances of the MEA prepared with 43% (Fig. 2(a)) or 20% Nafion (Fig. 2(b)) decreased faster than that with 33% Nafion (Fig. 1(a))

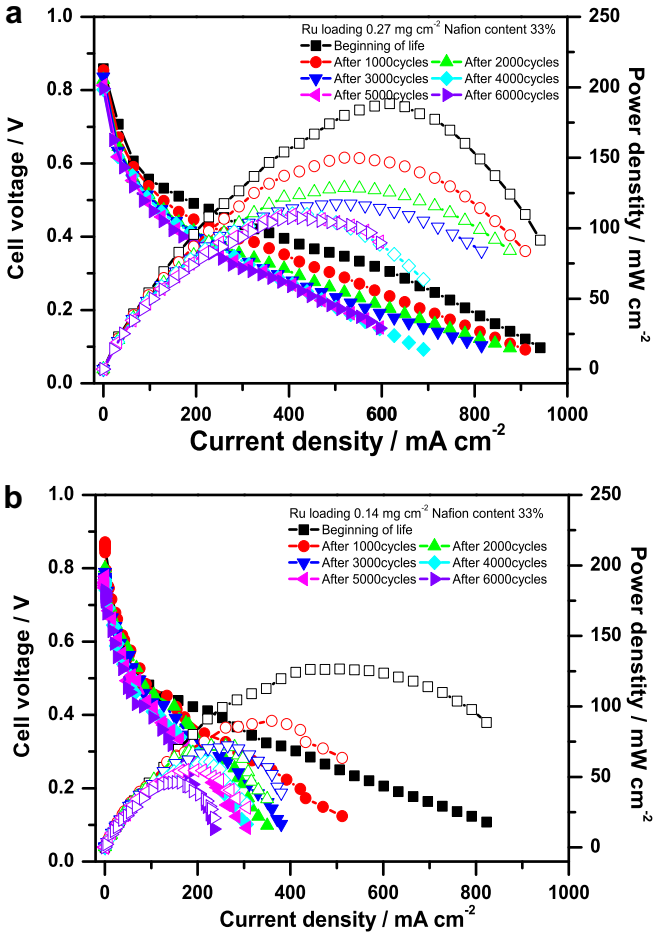

Fig. 1. Polarization and power density curves showing lifetime performances in the H_2/air single cell tests obtained at the optimized MEA fabrications (a) The maximum peak power density with 0.27 mg Ru cm^{-2} and 33% Nafion and (b) The best catalyst utilization with 0.14 mg Ru cm^{-2} and 33% Nafion. MEA: 5 cm^2, H_2/air: 100/250 ml min^{-1}, 65 °C; anode: 40 wt% Pt/C, 0.256 mg Pt cm^{-2}, Nafion 212; cathode: $Ru_{85}Se_{15}$/C.

during the ADTs upon 6000 cycles. While with 33% Nafion the lifetime performance of the MEA with 0.61 mg Ru cm^{-2} (Fig. 2(c)) was not as good as that at the optimized 0.27 mg cm^{-2} Ru (Fig. 1(a)), however, was much better than those obtained under other Ru and Nafion loads as seen in Fig. 1(b) and Fig. 2(a–b). It seemed that the amount of Nafion content more significantly affects the cell performance and durability. At the optimized 0.27 mg Ru cm^{-2}, variations in the Nafion contents from 20% to 43% resulted in very poor cell performance upon 6000 cycles.

3.2. Degradation diagnosis of fuel cell performance

The degree of performance degradation in fuel cells can be measured by the percentage loss in the maximum peak power density as defined below:

$$P_{loss} = \frac{P^0_{max} - P^{6000}_{max}}{P^0_{max}} \times 100 \quad (1)$$

The loss values for different Ru and Nafion loads are evaluated from Eq. (1) and are plotted against the cycle number in Fig. 3(a). At the same Ru loads, it is interesting to note from the left in Fig. 3(a) that either 43% or 20% Nafion contents led to the same amount of P_{loss} (80–82%) at the end of 6000 cycles. However, the 20% Nafion

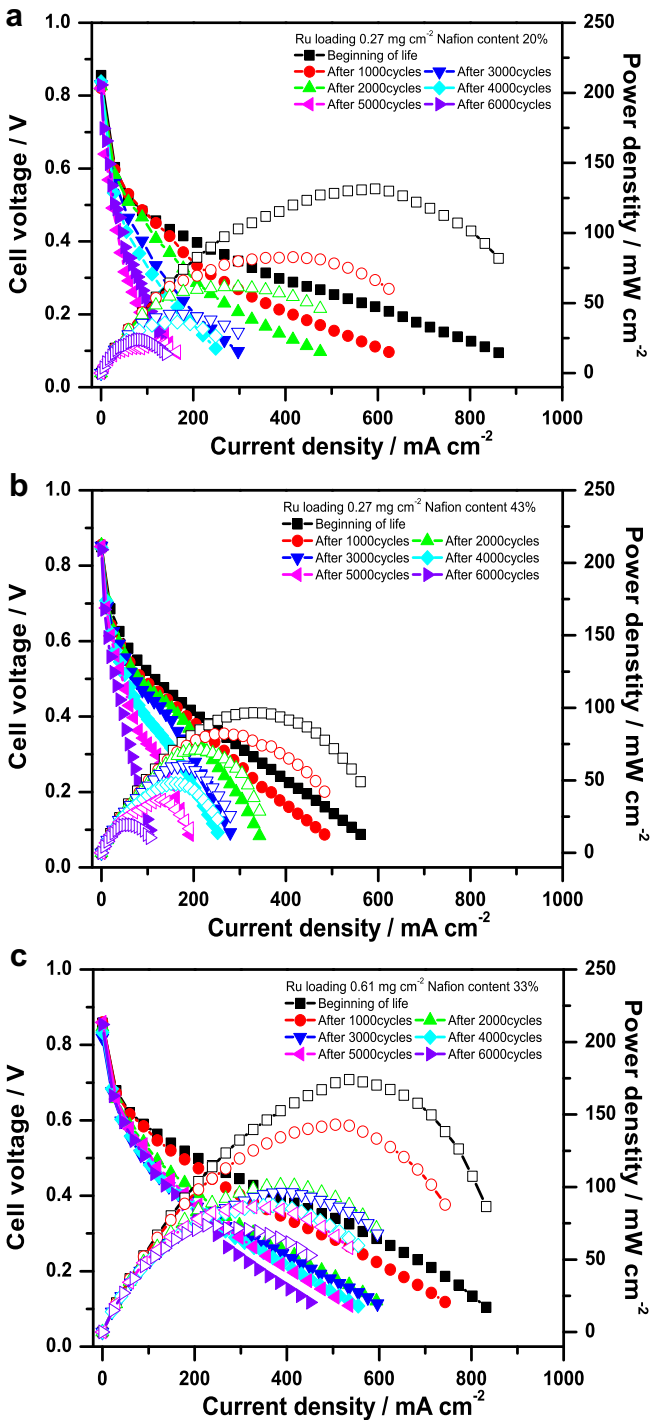

Fig. 2. Effects of Ru loadings and Nafion contents on lifetime performances in the H_2/air single cell tests. (a) 0.27 mg Ru cm^{-2} and 20% Nafion (b) 0.27 mg Ru cm^{-2} and 43% Nafion (c) 0.61 mg Ru cm^{-2} and 33% Nafion. MEA: 5 cm^2, H_2/air: 100/250 ml min^{-1}, 65 °C; anode: 40 wt% Pt/C, 0.256 mg Pt cm^{-2}, Nafion 212; cathode: $Ru_{85}Se_{15}$/C.

seemed to have more detrimental influence in lifetime performance, while the 43% Nafion showed almost linearly drops in power loss with the increase of cycle number. At the optimized 0.27 mg cm^{-2} Ru and 33% Nafion the apparent losses were observed upon 3000 cycles and then remained nearly unchanged afterward, which resulted in a total power loss of 44%. On the other hand, as illustrated in the right in Fig. 3(a), when using 33% Nafion the performance losses were less significantly affected by reducing Ru loads from 0.27 to 0.14 mg cm^{-2} or 0.61 mg cm^{-2}, which account for the total power losses of 64% and 57%, respectively.

The corresponding impedance data were collected at 0.4 V and are fitted using the equivalent circuit described previously [7], where R_Ω, R_{pt} and R_{ct} are the ohmic resistance, proton transfer resistance and charge transfer resistance, respectively. The results showing the effects of Nafion contents (left) and Ru loads (right) are compared in Fig. 3(b). The Nyquist plots showed semi-circular capacitive responses due to the pure hydrogen and high airflow, which lessen the anode and mass transport effect. The high frequency intercept with the real axis represents R_Ω, which is the total ohmic resistance of the cell including all the contact resistances between components and ohmic resistance of cell components such as the membrane, catalyst layers, GDLs, and bipolar plates. The low frequency intercept with the real axis is a measure of R_{ct}, which includes the charge transfer resistance of ORR and the mass transfer resistance [17]. The R_{pt} indicates proton transfer resistance within the catalyst layer. The impedance analysis results are consistent with the performance losses observed in Fig. 1(a), that is, the Nafion contents used for the preparation of the cathode catalyst layer in MEAs played a more dominant role in control of the lifetime performance. The values of three characteristic resistances for five representative Ru loads and Nafion contents before and after the ADTs are compared in Table 1. It is evident that all three characteristic resistances increased after the ADTs. The R_Ω value for the 43% Nafion was the largest before the ADTs, but changed little after the ADTs. The extremely large R_{ct} observed both before and after the ADTs among the five could be mainly responsible for the severe performance loss. On the other hand, the R_Ω values for the 20% Nafion and 0.61 mg Ru cm^{-2} became very large, while the R_{pt} for 0.14 mg Ru cm^{-2} was the largest after the ADTs.

The amounts of Nafion contents and Ru loads influenced the active site of catalyst, the channel of electron transfer and the three phase interface as they directly controlled the thickness of the cathode catalyst layer, accordingly significantly affected the cell performance [7]. To correlate the cell degradation to Nafion contents and Ru loads, it is necessary to analyze the MEAs before and after the ADTs.

3.3. Degradation analyses of MEAs

The membrane electrode assembly (MEA) is the key component of PEM fuel cells. Lifetime performance has been shown to be closely related to MEA performance [18]. Similar preparation procedures were used to obtain cross-sectional morphologies of MEAs before and after the ADTs. The cross-sectional SEM images of fresh and tested MEAs fabricated with 43% Nafion (at 0.27 mg Ru cm^{-2}) are compared in Fig. 4(a–b). The black and red curves in Fig. 4(a) were the line scans of the Ru and Pt elements, respectively, recorded along the fresh MEA, while the EDX spectra obtained in the anode and the cathode, as indicated in Fig. 4(b), are presented in Fig. 4(c–d). After the ADTs, both Se and Ru elements were detected in the anode (Fig. 4(c)), while almost no Se/Ru were left in the cathode (Fig. 4(d)), indicating a very severe Se/Ru migration from cathode to anode. The thickness of membrane decreased from 48 to 43 μm (approximately 10.4% shrinkage) and the cathode catalyst layer reduced from 16 to 10 μm, roughly 37.5% thinner (Fig. 4(b)). It was found that the high Nafion content in Pt/C catalyst layer would provide mass transfer pathways for contaminants (such as dissolved platinum and possibly iron) to diffuse into the membrane [19]. This might be the case in the current situation, which led to catalyst deactivation. The Se/Ru migrations were observed in all the other MEAs prepared with different Nafion contents and Ru loads. On the other hand, with the overloaded

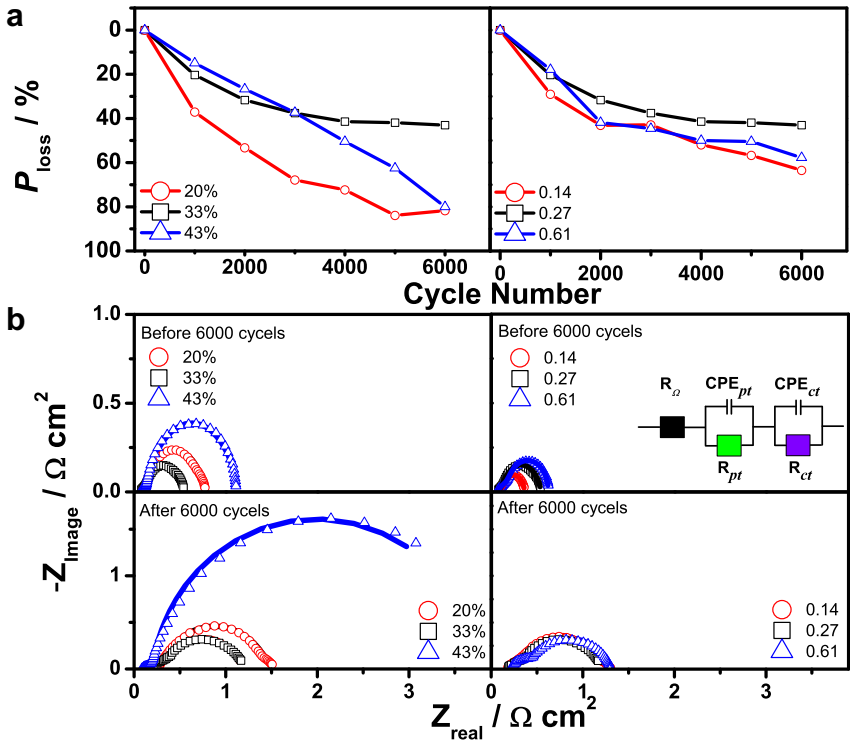

Fig. 3. (a) Performance loss as a function of power cycles and (b) Nyquist plots obtained under different catalyst loads and Nafion contents before and after 6000-cycle degradation. The inset in (b) shows the equivalent circuit used to fit the impedance data.

0.61 mg cm^{-2} (at 33% Nafion), the dissolution and migration of Se/Ru might become more seriously after the 6000 cycles degradation. The amounts of catalyst sites (the bright dots in Fig. 4(g)) decreased and the particle agglomeration became evident (Fig. 4(h)) due possibly to the delamination of Se/Ru from the catalyst and the corrosion of carbon support, which is responsible for the decayed performance observed in Figs. 1–2 or performance losses seen in Fig. 3(a).

Chemical degradation in the proton exchange membrane also influenced the lifetime cell performance [20]. To more quantitatively analyze the membrane degradation, the FTIR spectra were measured for both anode and cathode sides of membranes within MEAs before and after the ADTs. Fig. 5 illustrates a multiple curve fitting example of FTIR spectra obtained with the fresh and the anode/cathode sides of tested MEA prepared using 0.27 mg Ru cm^{-2} and 33% Nafion. As indicated in Fig. 5(a), the strong doublet IR bands observed at 1145 and 1208 cm^{-1} corresponded to C–F anti-symmetric vibrations contributed mainly from the backbone of Nafion membrane, while those appeared near 970 and 1056 cm^{-1} were assigned to C–O–C vibrations and S–O symmetric stretching vibration, respectively. A broad shoulder band seen around 1300 cm^{-1} belonged to anti-symmetric C–C stretching vibration [21,22]. The chemical degradation of Nafion membrane can be roughly evaluated by calculatingI_{1145}/I_{1205}, the ratio between the relative intensities associated with the C–F bonds, which is used to describe the backbone change in the membrane, and I_{1055}/I_{1205}, the ratio between the relative intensity associated with the S–O to C–F bonds, which is used to reflect the change of sulfonic acid in the membrane. The results are listed in Table 2. Compared with the fresh membranes (the values of I_{1145}/I_{1205} and I_{1055}/I_{1205} were 0.91 and 0.21, respectively), the I_{1145}/I_{1205} values for the anode and cathode sides of the tested membranes varied less than±2.53%, implying that the backbone of Nafion membranes is rather stable. However, the I_{1055}/I_{1205} values dropped more apparently, in particular, for the cathode side. The largest decreases of 19.3% and 9.43% were observed for the 43% Nafion in the cathode and the anode sides, respectively. This is consistent with the most severe membrane shrinkage (approximately 10%) observed in Fig. 4(a–b). It is believed that the overloaded Nafion presented in the catalyst layer would provide more pathways for the dissolution and migration of Se/Ru and the release of sulfonic acid, accordingly, this would cause the physical (shrinkage) and chemical (loss of sulfonic acid) degradation of the membrane.

Raman spectra were also obtained in order to investigate the degradation of carbon support. Fig. 6(a) supplies the Raman spectra obtained using the cathode catalyst layer prepared with 0.27 mg Ru cm^{-2} and 33% Nafion before and after the ADTs, as well as the carbon support $Ru_{85}Se_{15}$ catalyst and commercial Vulcan XC-72R carbon black powders. Two well-defined Raman bands corresponded to the D band of amorphous carbon and G band of graphitic carbon [7] were observed. The position of D band obtained with 325 nm Ultra-Violet Raman spectroscopy shifted from 1350 cm^{-1}–1430 cm^{-1} reported previously with 532 nm Nd:YAG laser Raman spectroscopy [7]. The values in relative intensity ratio of D to G bands (I_D/I_G) are calculated based on the

Table 1
Effects of Ru loads and Nafion contents on cell performances and three characteristic resistances before and after the accelerated degradation tests.

Catalyst layer		P_{loss} (%)	Resistances (Ω cm^2)					
Ru (mg cm^{-2})	Nafion (%)		R_Ω		R_{pt}		R_{ct}	
			Before	After	Before	After	Before	After
0.27	20	82	0.055	0.248	0.070	0.354	0.642	0.912
0.27	43	80	0.074	0.085	0.050	0.141	1.003	3.541
0.27	33	44	0.065	0.156	0.069	0.347	0.408	0.669
0.14	33	64	0.049	0.164	0.065	0.735	0.225	0.414
0.61	33	57	0.064	0.223	0.116	0.196	0.470	0.876

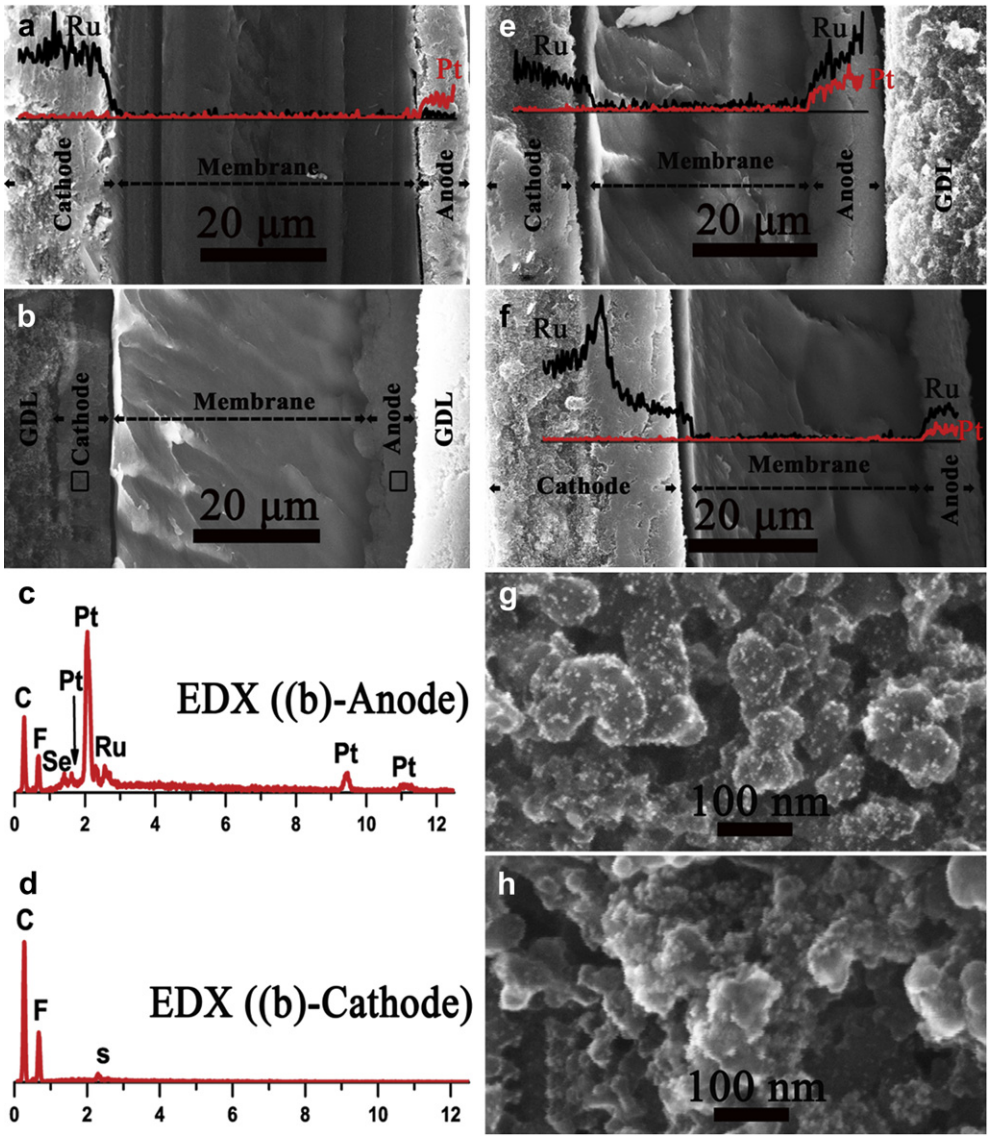

Fig. 4. Cross-sectional SEM images of (a) fresh and (b) tested MEAs (0.27 mg Ru cm^{-2} and 43% Nafion) and EDX spectra from (b): (c) anode (d) cathode. Cross-sectional SEM images of tested MEAs (e) 0.27 mg Ru cm^{-2} and 33% Nafion and (f) 0.61 mg Ru cm^{-2} and 33% Nafion. Surface morphologies of cathode catalyst layers with 0.61 mg Ru cm^{-2} and 33% Nafion (g) fresh (h) tested. The black and red curves in (a) (e) And (f) are scanned lines of EDX for Ru and Pt, respectively). (For interpretation of the references to colour in this figure legend, the reader is referred to the web version of this article.)

peak deconvolution of the Raman spectra and summarized in Table 3.

The obvious structure damage of carbon support has been observed after power cycles and start-up/shut down operations for automotive applications [23,24]. The rate of carbon corrosion in catalyst layer has been also enhanced by increasing the humidity of the electrochemical environment [25] and the platinum loading [24]. When carbon corrosion occurred, the dissolution and aggregation of Se/Ru might take place simultaneously in the catalyst layer. The Se/Ru might be more inclined to migrate into the membrane due to fewer carbon support and shorter path in the thinner catalyst layer. The degree of graphitization would decrease with the occurrence of carbon corrosion and increase with the Se/Ru dissolution and migration away from the carbon support. Therefore, the variations in I_D/I_G values, no matter whether increased (predominated by severe carbon corrosion) or decreased (predominated by the dissolutions and migrations of Se/Ru), would adversely influence cell performance and durability. The least 10.3% increase was observed with the optimized 0.27 mg Ru cm^{-2} and 33% Nafion, which led to only 44% performance loss after ADTs. The 30% decrease and 22% increase occurred with the underloaded 0.14 mg Ru cm^{-2} and overloaded 0.61 mg Ru cm^{-2}, respectively, while 16% decrease and 15% increase with the overloaded 43% Nafion and underloaded 20% Nafion, respectively. All these corresponded to more severe performance losses.

More structural insights of the $Ru_{85}Se_{15}$ nanoparticles can be obtained in TEM studies. The high resolution TEM images obtained from the catalyst layers before and after 6000 cycles are shown in Fig. 7(a–b) and Fig. 7(e–f), respectively. The $Ru_{85}Se_{15}$ nanoparticles in the fresh catalyst layer (Fig. 7(b)) were more uniformly distributed on carbon support than those in the tested catalyst layer (Fig. 7(f)) since the agglomeration of catalyst particles occurred after the ADTs. The selected area electron diffraction (SAED) patterns in Fig. 7(c) showed broad rings, indicating an amorphous-like RuSe structure for the fresh catalyst layer. After 6000 cycles of degradation, a lattice spacing of 0.206 nm can be clearly identified

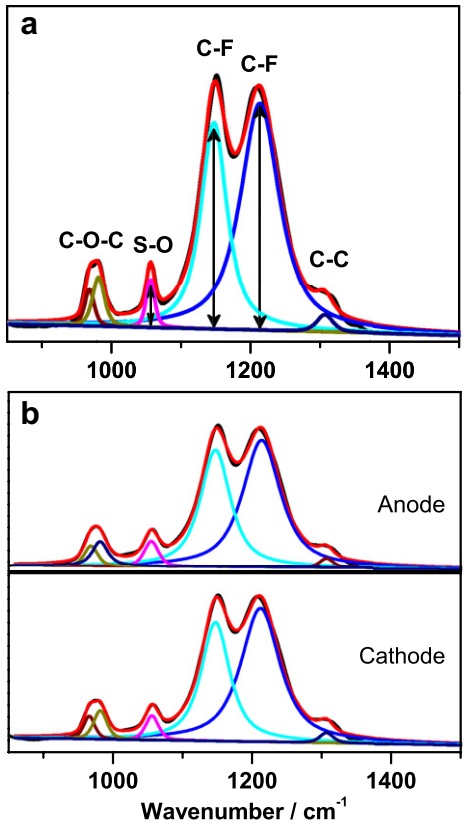

Fig. 5. FTIR spectra of the Nafion 212 membranes. (a) fresh (b) tested after ADTs for 6000 cycles. The identified peaks were deconvoluted by performing a multiple peak fitting procedure.

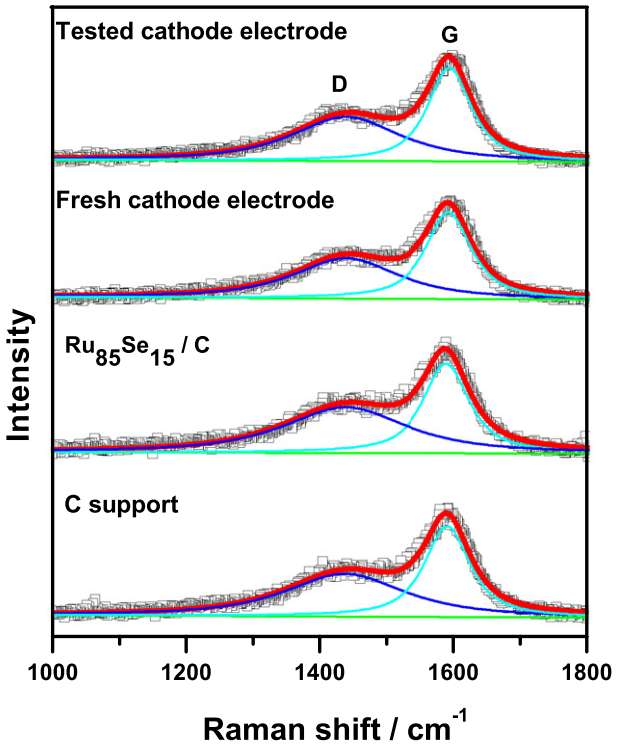

Fig. 6. Raman spectra of $Ru_{85}Se_{15}$/C cathode layers with different Ru and Nafion loads. The Raman spectra of $Ru_{85}Se_{15}$/C catalyst and carbon support are also included for comparisons.

as illustrated in the inset of Fig. 7(e). This is expected from the (101) lattice planes (0.2055 nm) of face-centered cubic (fcc) Ru. The bright spot appeared in the diffuse ring of SAED patterns in Fig. 7(g) is characteristic of polycrystalline, which is markedly different from the amorphous nature of fresh catalyst layer. The diameter of the diffuse ring is 9.73/nm, which is corresponding to Ru (101). The elements presented in the fresh and tested catalyst layers were identified to be Ru, Se and C from the corresponding EDX spectra (Fig. 7(d–h)), where Cu is an impurity from the copper grid used in the TEM analysis.

3.4. Degradation mechanism of $Ru_{85}Se_{15}$ catalyst layer in fuel cells

Based on the experimental results, the degraded performance in the H_2/air fuel cells obtained with the MEAs prepared using five representative Nafion contents and Ru loads could be resulted from the following four processes: (1) the dissolution and migration of Se/Ru from the cathode catalyst layer suggested from the observations of SEM/EDX (Fig. 4) and high resolution TEM/SAED (Fig. 7); (2) the loss of sulfonic acid in Nafion membrane implied from the FTIR analysis (Fig. 5 and Table 2); (3) the shrinkage of Nafion membrane evident in Fig. 4; and (4) the corrosion of carbon support indicated by the Raman analysis (Fig. 6 and Table 3). The Ru loads and Nafion contents used to prepare the MEAs would directly influence the thickness of the cathode catalyst layer, the amount of active sites, and the three phase interface.

The Ruthenium has good electrocatalytic activity toward ORR, which will be adversely influenced by its surface oxidation. To protect the Ru element from being oxidized, the Se element is introduced into $Ru_{85}Se_{15}$ [26]. However, Se was found to be easily oxidized at a potential as high as 0.85 V [27]. In the present case, the open circuit potential exceeded 0.85 V. Thus, Se might be oxidized to Se(IV) through electrochemical Reaction (2) or to SeO_2 by chemical Reaction (3).

$$Se^0 + 3H_2O = H_2SeO_3 + 4H^+ + 4e^- \quad (2)$$

$$Se^0 + O^2 = SeO_2 \quad (3)$$

The reversed Reaction (2) would take place at a potential lower than 0.85 V. The water soluble H_2SeO_3 formed by Reaction (2) could

Table 2
Effects of Ru loads and Nafion contents on chemical degradation of Nafion 212 membrane.

Catalyst layer		Membrane							
		Cathode				Anode			
Ru (mg cm^{-2})	Nafion (%)	I_{1145}/I_{1205}	Relative change (%)	I_{1055}/I_{1205}	Relative change (%)	I_{1145}/I_{1205}	Relative change (%)	I_{1055}/I_{1205}	Relative change (%)
0.27	20	0.887	−2.53	0.182	−14.2	0.918	+0.88	0.196	−7.55
0.27	43	0.902	−0.88	0.171	−19.3	0.897	−1.43	0.192	−9.43
0.27	33	0.927	+1.87	0.194	−8.49	0.896	−1.54	0.203	−4.24
0.14	33	0.918	+0.88	0.186	−12.3	0.917	+0.77	0.192	−9.43
0.61	33	0.909	+0.11	0.195	−8.02	0.920	+1.10	0.199	−6.13

Table 3
The I_D/I_G values calculated from Raman spectra for $Ru_{85}Se_{15}$/C, XC-72R and cathode catalyst layer prepared using different Ru loads and Nafion contents.

Parameter	I_D/I_G						
Ru (mg cm^{-2})	0.27	0.27	0.27	0.14	0.61	$Ru_{85}Se_{15}$/C	XC-72R
Nafion (%)	20	43	33	33	33		
Fresh	1.09	1.27	1.07	1.30	0.97	1.37	1.23
Tested	1.25	1.07	1.18	0.91	1.18		
$\Delta(I_D/I_G)$ (%)	+14.7	−15.7	+10.3	−30.0	+21.6		

be transferred into membrane or even further migrated to anode where the Se was apparently detectable by EDX as evident in Fig. 4(c). Similarly, the Ru crossover from cathode to anode was also observed after ADTs as seen in Fig. 4. In fact, this has been a case for all the MEAs tested in this study.

The surface of Ru_xSe_y catalyst is covered by Ru oxide (RuO_2) in the cathode through chemical oxidation reaction.

$$Ru + O_2 = RuO_2 \quad (4)$$

The RuO_2 presented at the surface of the Ru_xSe_y catalyst could be readily decomposed into Ru (IV) ions by reacting with dissolved H^+ in the water phase.

$$RuO_2 + 4H^+ = Ru^{4+} + 2H_2O \quad (5)$$

Part of Ru (IV) ions in the cathode could be further reduced to form metallic Ru according to

$$Ru^{4+} + 4e^- = Ru^0 \quad (6)$$

The formation of metallic Ru was verified by the presence of Ru (101) in the catalyst layers as indicated by TEM observation (Fig. 7), which might have a consequence to cause the catalyst aggregation. Other Ru (IV) ions had been transferred to the membrane and even migrated across the membrane to the anode, following the movement of water during fuel cell operation or of the Nafion ionomers distributed in the catalyst layer. Eventually, the Ru (IV) ions in the membrane phase or in the anode could be re-deposited as metallic Ru by reacting with hydrogen gas through the following reaction.

$$Ru^{4+} + 2H_2 \rightarrow Ru^0 + 4H^+ \quad (7)$$

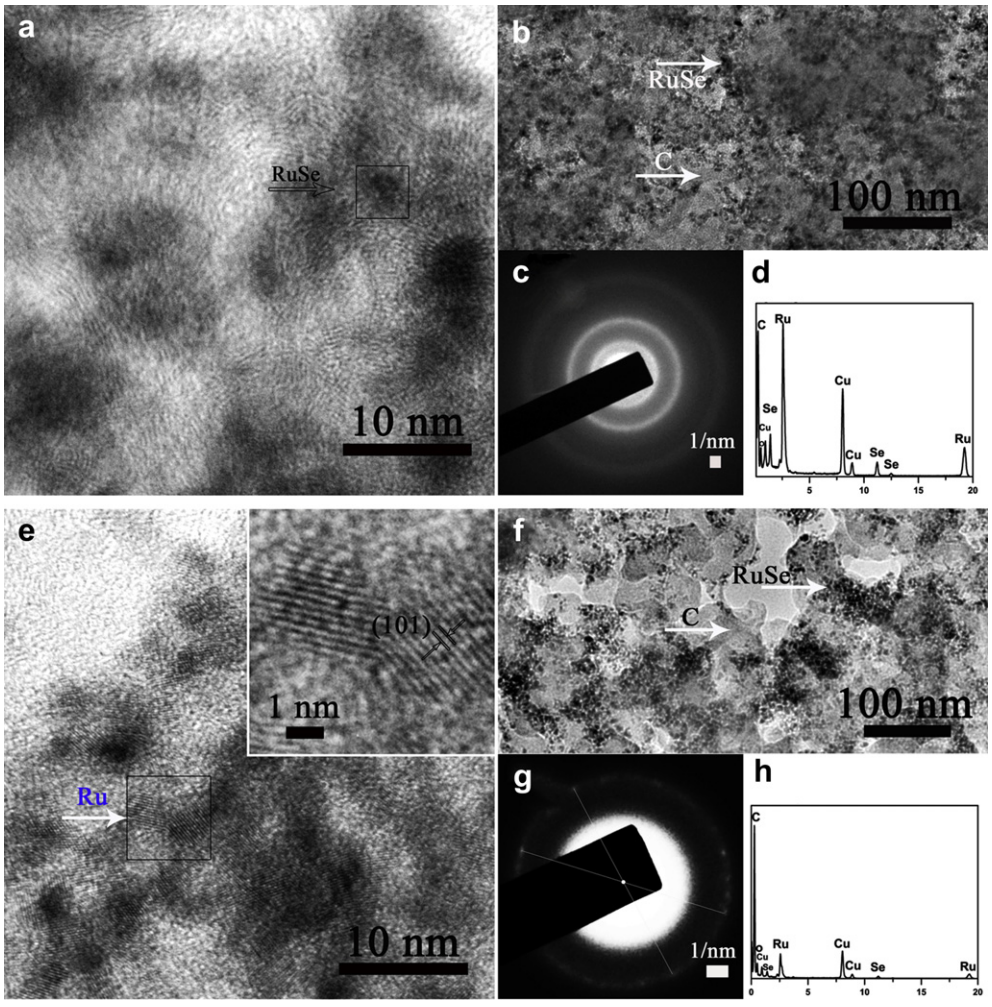

Fig. 7. HRTEM images, SAED patterns and EDX spectra of cathode catalyst layers with 0.27 mg Ru cm^{-2} and 33% Nafion: (a–d) fresh and (e–h) tested.

The electrochemical oxidation of metallic Ru, the reversed Reaction (6), would also take place at the anode and compete with hydrogen oxidation reaction, which results in more fuel consumption. Therefore, the dissolution and migration of both Se and Ru from the cathode catalyst layer directly lowered the catalyst activity, caused the carbon corrosion and the loss of sulfonic acid which induced the membrane shrinkage, all would detrimentally influence the cell performance and durability.

The Nafion contents used in the cathode catalyst layer play a more predominant role than Ru loads in fuel cell durability. The overloaded 43% Nafion in the cathode catalyst layer would lead to thicker catalyst layer and then heavier water flooding, which might simultaneously accelerate the dissolution and migration of Se and Ru (Fig. 4(a–d)), the serious membrane degradation including the apparent loss of sulfonic acid (Table 2) and membrane shrinkage (Fig. 4(a–b)), and the observed extremely large R_{ct} (Table 1); in contrast, the thinner catalyst layer formed by using underloaded 20% Nafion would provide a short path for Se/Ru migration across the membrane and rapid mass transport into the membrane or to the anode. The large R_{Ω} resulted by the carbon corrosion indicated with the 14.7% increase in I_D/I_G (Table 3) and R_{ct} due mainly to the losses of Se/Ru were observed. Both the overloaded and underloaded Nafion contents ultimately resulted in severe performance losses after the ADTs. On the other hand, although the thinner catalyst layer prepared with 0.14 mg Ru cm^{-2} led to the minimum R_{Ω} and R_{ct} (Table 1), the dissolution and migration of Se/Ru might become more detrimental to the active sites because of lower catalyst loading, indicated by the largest decrease of 30% in I_D/I_G (Table 3). The obvious loss of sulfonic acid (Table 2) might be responsible for the large R_{pt}. The thicker catalyst layer with 0.61 mg Ru cm^{-2} resulted in a large R_{Ω} (Table 1), the carbon corrosion became more serious as indicated by the large increase of 21.6% in I_D/I_G (Table 3), which probably slowed down mass transport and led to a large R_{ct}. It is, therefore, necessary to use the appropriate Nafion contents and Ru loads in cathode catalyst layer to improve cell performance and durability.

4. Conclusions

In the H_2/air single cells under the accelerated degradation tests (ADTs), the MEA fabricated at the optimized 0.27 mg Ru cm^{-2} and 33% Nafion resulted in the minor performance loss of 44%, while the MEAs with 43% and 20% Nafion contents at the same Ru load led to more than 80% losses upon 6000-cycle degradation. The initial dissolutions of Se/Ru from $Ru_{85}Se_{15}$ at the cathode catalyst layer and the subsequent migrations of Se/Ru across the membrane to the anode after the ADTs were confirmed with the experimental evidence provided by SEM/EDX and HRTEM/SAED analyses. The dissolutions and migrations of Se/Ru, resulted from the overloaded or underloaded Nafion contents and Ru loads, not only reduced the electroactive sites of the catalyst and caused the corrosion of carbon support, but also released the sulfonic acid and induced the membrane shrinkage, which ultimately lowered the lifetime performance of fuel cells. The Nafion contents used to prepare MEA seemed to be more critical than the Ru loads in control of cell durability since they determined the pathways for dissolutions and migrations of Se/Ru. The stabilities of Ru and Se in Ru_xSe_y seemed to have become critical in further improvements in activity and durability of Ru_xSe_y catalysts in order to make them competitive to Pt-based catalysts.

Acknowledgments

The authors wish to thank the financial support from the Fujian Key Laboratory of Advanced Materials, China (2006L2003). Mr. Zheng also greatly appreciates the graduate student scholarship provided by Xiamen University and Yuan Ze University under the student exchange program.

References

[1] T.R. Ralph, M.P. Hogarth, Platinum Met-Rev. 46 (2002) 3–14.
[2] J. Wu, X.Z. Yuan, J.J. Martin, H. Wang, J. Zhang, J. Shen, S. Wu, W. Merida, J. Power Sources 184 (2008) 104–119.
[3] Y. Feng, A. Gago, L. Timperman, N. Alonso-Vante, Electrochim. Acta 56 (2011) 1009–1022.
[4] N. Alonso-Vante, H. Tributsch, Nature 323 (1986) 431–432.
[5] G. Liu, H. Zhang, J.W. Hu, Electrochem Commun. 9 (2007) 2643–2648.
[6] Q. Zheng, X. Cheng, T.-C. Jao, F.-B. Weng, A. Su, Y.-C. Chiang, Int. J. Hydrogen Energy 36 (2011) 14599–14607.
[7] Q. Zheng, X. Cheng, T.-C. Jao, F.-B. Weng, A. Su, Y.-C. Chiang, J. Power Sources 201 (2012) 151–158.
[8] R.G. González-Huerta, A. Guzman-Guzman, O. Solorza-Feria, Int. J. Hydrogen Energy 35 (2010) 12115–12119.
[9] K.-T. Jeng, N.-Y. Hsu, C.-C. Chien, Int. J. Hydrogen Energy 36 (2011) 3997–4006.
[10] D. Seo, J. Lee, S. Park, J. Rhee, S.W. Choi, Y.-G. Shul, Int. J. Hydrogen Energy 36 (2011) 1828–1836.
[11] C.G. Chung, L. Kim, Y.W. Sung, J. Lee, J.S. Chung, Int. J. Hydrogen Energy 34 (2009) 8974–8981.
[12] A.C. Fernandes, E.A. Ticianelli, J. Power Sources 193 (2009) 547–554.
[13] R. Lin, B. Li, Y.P. Hou, J.M. Ma, Int. J. Hydrogen Energy 34 (2009) 2369–2376.
[14] S. Zhang, X.-Z. Yuan, J.N.C. Hin, H. Wang, K.A. Friedrich, M. Schulze, J. Power Sources 194 (2009) 588–600.
[15] N. Yousfi-Steiner, P. Moçotéguy, D. Candusso, D. Hissel, J. Power Sources 194 (2009) 130–145.
[16] T. Xu, H. Zhang, H. Zhong, Y. Ma, H. Jin, Y. Zhang, J. Power Sources 195 (2010) 8075–8079.
[17] C.S. Kong, D.-Y. Kim, H.-K. Lee, Y.-G. Shul, T.-H. Lee, J. Power Sources 108 (2002) 185–191.
[18] X. Cheng, L. Chen, C. Peng, Z. Chen, Y. Zhang, Q. Fan, J. Electrochem. Soc. 151 (2004) A48–A52.
[19] A.P. Young, J. Stumper, S. Knights, E. Gyenge, J. Electrochem. Soc. 157 (2010) B425–B436.
[20] X. Cheng, C. Peng, M. You, L. Liu, Y. Zhang, Q. Fan, Electrochim. Acta 51 (2006) 4620–4625.
[21] S.R. Lowry, K.A. Mauritz, J. Am. Chem. Soc. 102 (1980) 4665–4667.
[22] W. Kujawski, Q.T. Nguyen, J. Neel, J. Appl. Polym. Sci. 44 (1992) 951–958.
[23] K. Malek, A.A. Franco, J. Phys. Chem. B 115 (2011) 8088–8101.
[24] A.A. Franco, M. Gerard, J. Electrochem. Soc. 155 (2008) B367–B384.
[25] D.A. Stevens, A.M.T. Hicks, A.G.M. Haugen, A.J.R. Dahn, J. Electrochem. Soc. 152 (2005) A2309–A2315.
[26] H. Cheng, W. Yuan, K. Scott, D.J. Browning, J.B. Lakeman, J. Power Sources 172 (2007) 597–603.
[27] M. Solaliendres, A. Manzoli, G. Salazar-Banda, K. Eguiluz, S. Tanimoto, S. Machado, J. Solid State Electrochem. 12 (2008) 679–686.